

Illusions of Self-Motion during Magnetic Resonance-Guided Focused Ultrasound Thalamotomy for Tremor

Matteo Ciocca, MD ¹, Ayesha Jameel, MD ², Nada Yousif, PhD ³, Neekhil Patel, PhD,¹
Joely Smith, MSc ⁴, Sena Akgun, MB ², Brynmor Jones, MD,²
Wlaysia Gedroyc, MD, MRCP, FRCR,² Dipankar Nandi, MD, PhD ¹,
Yen Tai, MD, PhD ¹, Barry M. Seemungal, MD, PhD ¹ and
Peter Bain, MD (Res), FRCP ¹

Objective: Brain networks mediating vestibular perception of self-motion overlap with those mediating balance. A systematic mapping of vestibular perceptual pathways in the thalamus may reveal new brain modulation targets for improving balance in neurological conditions.

Methods: Here, we systematically report how magnetic resonance-guided focused ultrasound surgery of the nucleus ventralis intermedius of the thalamus commonly evokes transient patient-reported illusions of self-motion. In 46 consecutive patients, we linked the descriptions of self-motion to sonication power and 3-dimensional (3D) coordinates of sonication targets. Target coordinates were normalized using a standard atlas, and a 3D model of the nucleus ventralis intermedius and adjacent structures was created to link sonication target to the illusion.

Results: A total of 63% of patients reported illusions of self-motion, which were more likely with increased sonication power and with targets located more inferiorly along the rostrocaudal axis. Higher power and more inferiorly targeted sonications increased the likelihood of experiencing illusions of self-motion by 4 and 2 times, respectively (odds ratios = 4.03 for power, 2.098 for location).

Interpretation: The phenomenon of magnetic vestibular stimulation is the most plausible explanation for these illusions of self-motion. Temporary unilateral modulation of vestibular pathways (via magnetic resonance-guided focused ultrasound) unveils the central adaptation to the magnetic field-induced peripheral vestibular bias, leading to an explicable illusion of motion. Consequently, systematic mapping of vestibular perceptual pathways via magnetic resonance-guided focused ultrasound may reveal new intracerebral targets for improving balance in neurological conditions.

ANN NEUROL 2024;00:1–12

Magnetic resonance imaging-guided focused ultrasound (MRgFUS) is a noninvasive and precise technique used to treat tremor in conditions such as essential

tremor (ET) and Parkinson disease (PD). By delivering thermal energy to the targeted area, typically the nucleus ventralis intermedius (VIM) of the thalamus, MRgFUS

View this article online at [wileyonlinelibrary.com](https://www.wileyonlinelibrary.com). DOI: 10.1002/ana.26945

Received Dec 12, 2023, and in revised form Apr 16, 2024. Accepted for publication Apr 17, 2024.

Address correspondence to Dr Ciocca, Division of Brain Sciences, Department of Neurosciences, Imperial College London, London, United Kingdom. E-mail: m.ciocca20@imperial.ac.uk. Dr Seemungal, Division of Brain Sciences, Department of Neurosciences, Imperial College London, London, United Kingdom. E-mail: b.seemungal@imperial.ac.uk. Dr Bain, Division of Brain Sciences, Department of Neurosciences, Imperial College London, London, United Kingdom. E-mail: p.bain@imperial.ac.uk

Barry M. Seemungal and Peter Bain are joint senior authors.

From the ¹Department of Brain Sciences, Charing Cross Hospital, Imperial College London, London, United Kingdom; ²Department of Radiology, St Mary's Hospital, Imperial College Healthcare NHS Trust, London, United Kingdom; ³School of Engineering and Computer Science, University of Hertfordshire, Hatfield, United Kingdom; and ⁴Faculty of Engineering, Department of Bioengineering, Imperial College London, London, United Kingdom

Additional supporting information can be found in the online version of this article.

creates a lesion that disrupts the abnormal neural activity responsible for tremor, resulting in significant symptom reduction.^{1,2} Currently, MRgFUS thalamotomy is widely used for the treatment of neuropathic pain, essential tremor, and parkinsonian tremor.²

The thalamus serves as a cortical relay station in the vestibular network, receiving afferent inputs from the periphery and transmitting them to the cerebral cortex.³ The vestibular system, in combination with other sensory and motor systems, mediates several ecological functions, from ocular and postural stability to self-motion perception and spatial orientation.^{4,5} Recent data show that vestibular cortical networks mediating self-motion perception and postural control are partially overlapping.⁶ Overlap between perception and postural control has been identified in the inferior longitudinal fasciculus⁷ and in the ventral lateral nucleus of the thalamus.⁸ Notably, in patients with PD, stimulation of the dentatothalamic pathway using deep brain stimulation (DBS) can elicit the perception of rotational motion.⁸ The dentatothalamic pathway carries signals of angular head rotation from the semicircular canals as well as convergent signals mediating combined canal and linear acceleration from the otoliths to the ventral lateral nucleus of the thalamus.⁸ Electrical stimulation of the VIM during radiofrequency thalamotomy in humans has evoked vestibular sensations of a movement through space.^{9,10}

In a previous study of 14 patients with ET, 7 patients reported that they felt as if they were being transiently tilted in the pitch plane with their head down and legs up during the MRgFUS procedure.¹¹ Similar symptoms were also reported by other groups, who described a sensation of tilting, falling, or spinning in 33% of patients,¹² and a transient “dizziness” or “vertigo” has been described by approximately 20 to 40% of patients in other trials.^{13–15} However, in a comprehensive safety analysis involving 186 patients with tremor, no instances of sonication-related dizziness, vertigo, or sensations of motion through space were documented.¹⁶ Therefore, critically, the illusion of self-motion described by patients undergoing MRgFUS has not been systematically characterized, which is a potentially important omission, because the recently described overlap between brain mechanisms mediating human postural control and vestibular perception of self-motion indicates that a detailed mapping of central vestibular regions may provide novel targets for brain modulation to treat imbalance and falls in patients with brain disease.

We herein map vestibular-perceptual illusions provoked by MRgFUS by systematically recording the illusions of self-motion reported by patients with ET and/or PD while in the magnetic resonance imaging (MRI) scanner undergoing MRgFUS thalamotomy for tremor. We

collected detailed descriptions of these illusory body movements, to better understand their characteristics and similarities with previously described vestibular illusions. Additionally, we propose a mechanistic model that explains these illusions, incorporating (1) stimulation intensity-related effects and (2) anatomical localization of cerebellar–thalamic pathways mediating body and body-part motion signaling. We additionally explain the main plane of illusory self-motion by combining the effect of MRgFUS and the phenomenon of magnetic vestibular stimulation involving Lorentz force-mediated magnetic field stimulation of the peripheral vestibular apparatus.

Patients and Methods

Patient Selection

In view of the unique nature of this transient effect, we assessed the occurrence of this phenomenon in a cohort of 46 patients treated with MRgFUS for ET, Parkinson tremor, or both. Of these patients, 12 were retrospectively reviewed (MRgFUS thalamotomy between March 2019 and September 2021) and 34 cases were prospectively evaluated (MRgFUS between October 2021 and August 2022).

Patients aged >18 years with moderate or severe ET, Parkinson tremor, or both, causing significant disability and with an inadequate response to medication, were eligible for MRgFUS providing that they met standard inclusion criteria and did not have any exclusion criteria.¹¹ Importantly, the criteria for exclusion include any past history of a peripheral/central vestibular dysfunction and the presence of any sign of a peripheral vestibular dysfunction during the preoperative assessment. The study was approved by the UK Health Research Authority (IRAS ID 255217; study sponsor Imperial College London), enabling pseudonymized data to be accessed postoperatively. Patients signed a written consent form before undergoing the MRgFUS procedure. Demographic, clinical, and technical details of the entire MRgFUS treatment were collected as per our standard of procedure. The study was performed in accordance with the Declaration of Helsinki.

MRgFUS Treatment

The MRgFUS technique deployed is described in detail in a previous publication¹¹ and in Supplementary Materials, Methods.

Phenomenology of Illusory Body Motion

All patients were assessed before the beginning of the procedure and then after each sonication for tremor improvement, and adverse effects were collected as previously described.¹¹ Patients were not specifically prewarned about the possibility of experiencing dizziness during the

procedure, as our standard informed consent process did not include explicit mention of dizziness due to the absence of any prior reports of unpleasant or alarming dizziness in our patient population, which is consistent with the existing literature. During the planning phase, patients lay down on the MRI bed with the stereotactic frame attached to the MRgFUS transducer. This phase lasts approximately 1 hour. We interrogated patients about any sensations that they may have experienced at the end of this phase. Then, during the sonication phase, and specifically about 30 to 60 seconds after every sonication, patients were asked whether any sensation was experienced and if so to describe it to us. A self-reported description of the episode was recorded immediately after each sonication for every patient (see Supplementary Materials, Table S2).

As a common, reliable nomenclature to describe the illusion of self-motion is essential for interpreting patients' reports, we initially reached an internal consensus on how to classify the illusions of self-motion, which were categorized into (1) rotations (ie, semicircular canal-mediated pathways), (2) translations (otolith-mediated movements), and (3) mixed rotation–translation. Rotations were subdivided according to the main axis of rotation by using a gravity-referenced coordinate system. Therefore, we classified yaw as a rotating sensation orthogonal to gravity, roll as a rotating sensation in the frontal plane around an anteroposterior axis (ie, a left over right or right over left shoulder movement), and pitch as a rotating sensation in the sagittal plane perpendicular to the gravity axis (ie, head-over-heels or heels-over-head rotation; Fig 1). This nomenclature is derived from the vestibulo-ocular reflex

nomenclature, which is commonly used in neuroanatomical studies on the vestibular network.¹⁷

Illusion of Self-Motion and MRgFUS Characteristics

To support our hypothesis of a power-dependent illusion of self-motion, we systematically collected data on the power and maximum temperature achieved during each sonication for each target for each patient. Power values have been analyzed as raw values and as normalized values, as previously described by Segar and colleagues (see Supplementary Materials, Methods).¹⁸

We then compared MRgFUS power and maximum temperature for (1) sonications with and without illusion of self-motion; (2) sonications with rotations, translation, and mixed rotation–translation; and (3) sonications with illusory rotation, by subdividing them based on the main axis of perceived rotation.

Finally, we subdivided targets into 3 different groups, based on the appearance of an illusion of self-motion related to an increase in the power of sonications. The first group consisted of targets where increasing the sonication power always triggered an illusion of self-motion, even at lower power values. The second group encompassed targets where sonications did not trigger any illusion at low power, but patients reported an illusion for higher power values (ie, a power-dependent illusions of self-motion). Finally, the third group included targets where sonications did not trigger an illusion. For this part, we only included data from patients from the prospective group.

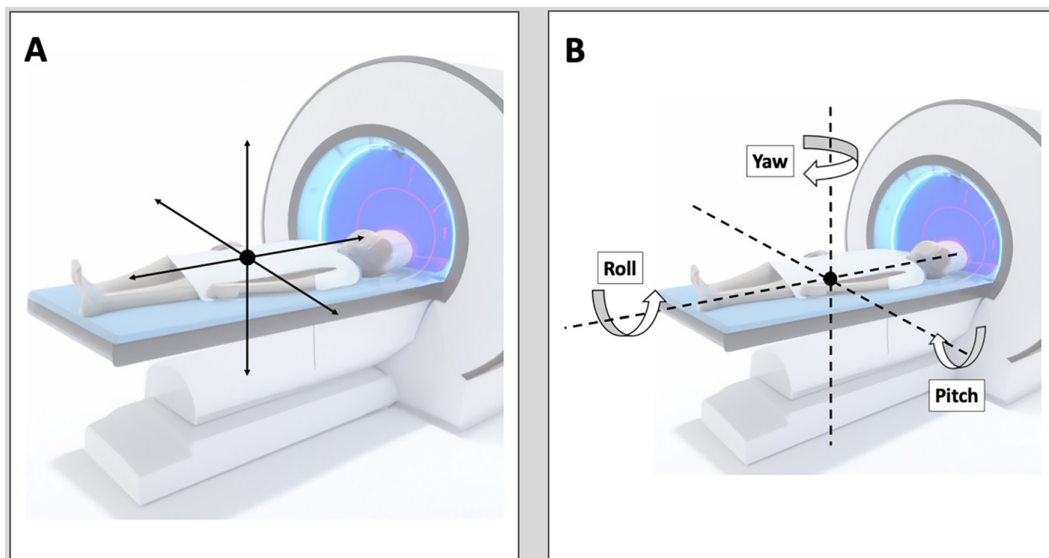


FIGURE 1: Graphic representation of the nomenclature of illusion of self-motion. (A) Translational movements, which encompass the illusion of body translation in one or more directions along 3 main axes. (B) Rotational movements, which include a rotation along one or more of the 3 axes, with a center of rotation at the level of the pelvis and an observation frame of reference based on gravity. Illusion of self-motion may happen as in A, B, or as a combination of A and B.

Mapping the Vestibular Network within the VIM and Adjacent Structures

As we hypothesize that anatomical localization of the sonication target along the cerebellar–thalamic pathways is essential to mediate the illusory body and body-part motion, cartesian coordinates of each sonication target were collected and normalized (see Supplementary Materials, Methods). To corroborate our hypothesis, we initially predicted that sonications located more inferiorly in the posterior subthalamic area (PSA) were more likely to evoke an illusory self-motion, as the cerebellothalamic tract is not as dispersed as in VIM. Therefore, we initially focused on patients who had received treatment in multiple targets and reported experiencing no illusion at one target and an illusion at another, and we compared their standardized coordinates for the 3 axes. Then, we compared targets that did not evoke any illusion to targets where the illusion was always present regardless of the magnitude of power used to sonicate.

Finally, we also compared the standardized coordinates for each target evoking an illusion of translation, rotation, or both, and targets with illusions of rotational movements along different axes.

Visualization of Targets in the VIM/PSA

To gain a deeper understanding of the thalamic structures and circuits involved in illusory self-motion, we optimized the visualization of the averaged target for each group by utilizing an atlas-based 3-dimensional (3D) model (see Supplementary Materials, Methods for further details).^{19,20}

Statistical Methods

Statistical analysis was performed with SPSS version 26. Two-sided *t* tests were employed for univariate analysis to examine potential contributors to the illusion of self-motion. One-way analysis of variance with multiple comparison correction (Bonferroni correction) was performed to compare more than 3 groups. Results are presented as mean \pm standard deviation. A binary logistic regression analysis has been performed to estimate odds ratios (ORs) for the illusion of movement.

Results

Patient Demographics

The demographics of the patients studied are shown in Table 1 and Supplementary Materials, Table S1. We separated patients into 2 cohorts, a retrospective cohort and a prospective cohort, based on data sampling. The 2 cohorts were analyzed independently. There were no statistically significant differences in demographics between these 2 groups (Table 1).

Phenomenology of Illusory Self-Motion

Data are reported in detail in Supplementary Materials, Tables S2–S4. Briefly, none of the patients reported dizziness, vertigo, or illusion of self-motion at the end of the planning phase. A total of 29 of the 46 patients (63%) reported at least one sensation of movement during MRgFUS treatment, 4 of 12 patients (33.3%) in the retrospective group, and 25 of 34 patients in the prospective group (73.5%). Of the 29 patients who experienced an illusion, 18 patients experienced only one kind of illusion of self-motion (62.1%), whereas the remaining 11 experienced 2 or more different illusions (37.9%). Based upon patients' descriptions (Fig 1), we identified 22 patients who experienced a rotational illusion (75.8%), 2 with a translation (6.9%) and 5 with a combined rotation/translation illusion (17.3%).

Characteristics of Illusory Self-Motion

Patient Demographics. We compared demographic characteristics of patients with and without illusory self-motion in the retrospective and prospective cohorts, and results are reported in Supplementary Materials, Table S6. No significant differences between the 2 groups were noted.

MRgFUS Characteristics

Anatomical Features. The skull density ratio (SDR) and the anterior commissure (AC)–posterior commissure (PC) length for each patient are shown in the Supplementary Materials, Table S3. The mean SDR and AC-PC line length did not differ between the groups with and without illusory self-motion (Table 2).

MRgFUS Parameters. MRgFUS parameters for each patient are reported in the Supplementary Materials, Table S3. As our hypothesis was that an illusory self-motion is evoked by higher power sonications, we compared power and maximum temperature between sonications with and without illusory self-motion in the prospective cohort using the independent *t* test comparison. The 2 groups did not differ in terms of maximum temperature ($t = -1.041$, $p = 0.298$), but a significant difference in power was observed after multiple comparison correction, with the "movement group" showing slightly higher power output ($t = -2.409$, $p = 0.017$; Table 2).

To provide additional evidence regarding the influence of sonication power in eliciting an illusion of self-motion, we divided the power values into quartiles and calculated the proportion of sonications that induced the phenomenon for each quartile. The results reveal a progressive increase in the proportions of sonications evoking an illusory self-motion, ranging from 38.9% in the 1st

TABLE 1. Comparison of the Demographic Details of Patients in the Restrospective and Prospective Cohorts

Characteristic	Retrospective Cohort	Prospective Cohort	Total
Patients, n	12	34	46
Age, yr	70.3 (58–82)	72.7 (61–84)	72.09 (58–84)
Gender	9 M, 3 F	26 M, 8 F	35 M, 11 F
Handedness	12 RH	29 RH, 5 LH	41 RH, 5 LH
Diagnosis	7 ET (58.3%)	28 ET (82.4%)	35 ET (76.1%)
	4 PT (33.3%)	5 PT (14.7%)	9 PT (19.5%)
	1 ET/PT (8.4%)	1 ET/PT (2.9%)	2 ET/PT (4.4%)
Duration of tremor: ET	41.9 (8–61)	32.1 (7–63)	34.3 (7–63)
Duration of tremor: PD	6.4 (3–9)	13 (3–31)	9.2 (3–31)
Arm treated	12 R	27 R, 7 L	39 R, 7 L
Targets per patient	2.66 (2–6)	2.29 (2–5)	2.39 (2–5)
Sonications per patient	6.08 (4–11)	4.26 (2–11)	5.17 (2–11)
Sonication-per-target ratio	2.28	1.86	2.22

For age, duration of tremor, targets per patient, and sonications per patient, the range of values is reported. For diagnosis, the percentage of each diagnosis of the total is reported.

ET = essential tremor; F = females; L = left; LH = left-handed; M = male; PD = Parkinson disease; PT = Parkinsonian tremor; R = right; RH = right-handed.

quartile (representing low power) to 53.2% in the 4th quartile (representing high power). This trend is visually represented in Supplementary Materials Figure S1, which displays a proportional distribution across the 2 categories of illusion of self-motion and no movement. This difference is also present when comparing power values normalized for the individual SDR ($t = -3.032$, $p = 0.003$).

By looking at how the sonication power influenced the illusory self-motion, we identified three different possible behavioral responses, namely movement at any power value, movement only at high power values, and no movement. Accordingly, we subdivided the targets into (1) targets where sonications always trigger an illusion of self-motion, (2) targets where sonications triggered an illusion of self-motion only after increasing the power, and (3) targets where sonications did not trigger any illusion. As this subdivision requires a systematic and detailed collection of movement characteristics, we limited our analysis to the prospective cohort. Results are reported in detail in Supplementary Materials, Table S7. We observed a statistically significant difference in power ($F = 5.389$, $p = 0.005$) between targets where sonications triggered an illusion of self-motion only after increasing the power and the other 2 groups. We also observed that sonications evoking power-dependent illusions had a lower minimum

power ($F = 5.006$, $p = 0.009$) compared with sonications from the other groups (ie, after Bonferroni correction, $p = 0.012$ for sonications always triggering an illusion and $p = 0.02$ for sonications with no illusion).

No statistically significant difference in any of the MRgFUS parameters was found between translational, rotational, and a combination of translational and rotational movements (Supplementary Materials, Table S4) and within rotational movements stratified by the main axis of rotation (Supplementary Materials, Table S5).

Target Locations

Results are reported in detail in Table 2 and Supplementary Materials Tables S3–S5, and S7; as both standardization procedures led to similar results, we report here only results normalized on the average AC-PC line from our patient group.

Initially, we focused on patients who had received treatment in multiple targets and reported experiencing no illusion in one target and an illusion in another. We identified 4 patients, with a total of 5 targets for each group. A statistically significant difference along the z-axis was noted, as targets with illusions of self-motion were located more inferiorly (no movement: $+1.4040 \pm 0.92$, movement: -1.27 ± 0.66 ; $F = 1.271$, $p = 0.001$). We

TABLE 2. Comparison of MRgFUS Characteristics between Sonications with and without the Associated Illusion of self-motion and of Target Coordinates between Targets with and without the Associated Illusion of self-motion in the Prospective Cohort

MRgFUS Characteristics	No Movement	Movement	<i>p</i>
Anatomical Features			
SDR	0.51 (0.11)	0.54 (0.12)	0.385
AC-PC length, mm	27.53 (1.55)	27.52 (1.53)	0.989
MRgFUS parameters			
Sonications, total number	131	106	
Energy, J	10,537.62 (5,992)	10,644.53 (5,741.4)	0.889
Time, s	16.51 (5.78)	15.68 (5.83)	0.274
Average temperature, °C	53.03 (3.98)	53.62 (3.62)	0.38
Maximum temperature, °C	56.60 (4.47)	57.20 (4.41)	0.299
Power, W	600.54 (175.70)	653.27 (156.82)	0.017*
Target coordinates			
Targets, total number	26	50	
x, mm	15.22 (1.65)	14.67 (1.80)	0.188
y, mm	-5.04 (1.25)	-5.02 (0.93)	0.934
z, mm	0.83 (1.33)	0.22 (1.68)	0.093

Coordinates have been scaled to the averaged AC-PC line from our cohort of patients. Mean and standard deviation (in parentheses) are reported. A statistically significant difference in power (*) and a trend toward a statistically significant difference in target localization along the z-axis have been observed ($p = 0.017$ and $p = 0.093$, respectively).

AC = anterior commissure; MRgFUS = magnetic resonance imaging-guided focused ultrasound; PC = posterior commissure; SDR = skull density ratio.

represented this difference in our model by building a vector of the movement, from the “no illusion of self-motion” target to the “illusion of self-motion” target. The model shows consistent and uniform movement vectors in all patients (Fig 2).

As the location of the target along the z-axis appeared to be critically important as a determinant of the occurrence of an illusion of self-motion, we investigated the distribution of targets with and without an evoked illusion along the z-axis. To do so, we subdivided our targets into quartiles, and we observed how the illusion of self-motion was more constantly reported in inferior targets (1st and 2nd quartiles) than in more superior targets (3rd and 4th quartiles; Fig 3). To better visualize the differences between our targets, we incorporated our coordinates into the 3D atlas-based model and observed that the lower targets (below the 2nd quartile) are located in the PSA, whereas the higher targets (above the 2nd quartile) are located in the VIM (Fig 4).

As the median value of our targets is located on the AC-PC line plane, we decided to collate the 1st and the 2nd quartiles, which encompass all the targets above the AC-PC plane (ie, in the VIM), and all the targets below the AC-PC plane (3rd and 4th quartiles, ie, in the PSA). We then compared the coordinates of targets with and without an illusory self-motion for targets above and below the AC-PC line by means of independent *t* tests. Results are reported in Table 3. More inferior coordinates are more likely to evoke an illusion of self-motion (no movement: -0.9957 ± 0.05 , movement: -1.38 ± 0.72 ; $t = 2.538$, $p = 0.018$), whereas no differences in power were noted both in the PSA and in the VIM. Therefore, targets which are located inferiorly in the PSA are likely to evoke an illusory self-motion independently of the magnitude of power used to sonicate them.

To further support the relevance of the location along the z-axis, we investigated whether any difference was present between targets where an illusion was always present and targets where an illusion was never evoked,

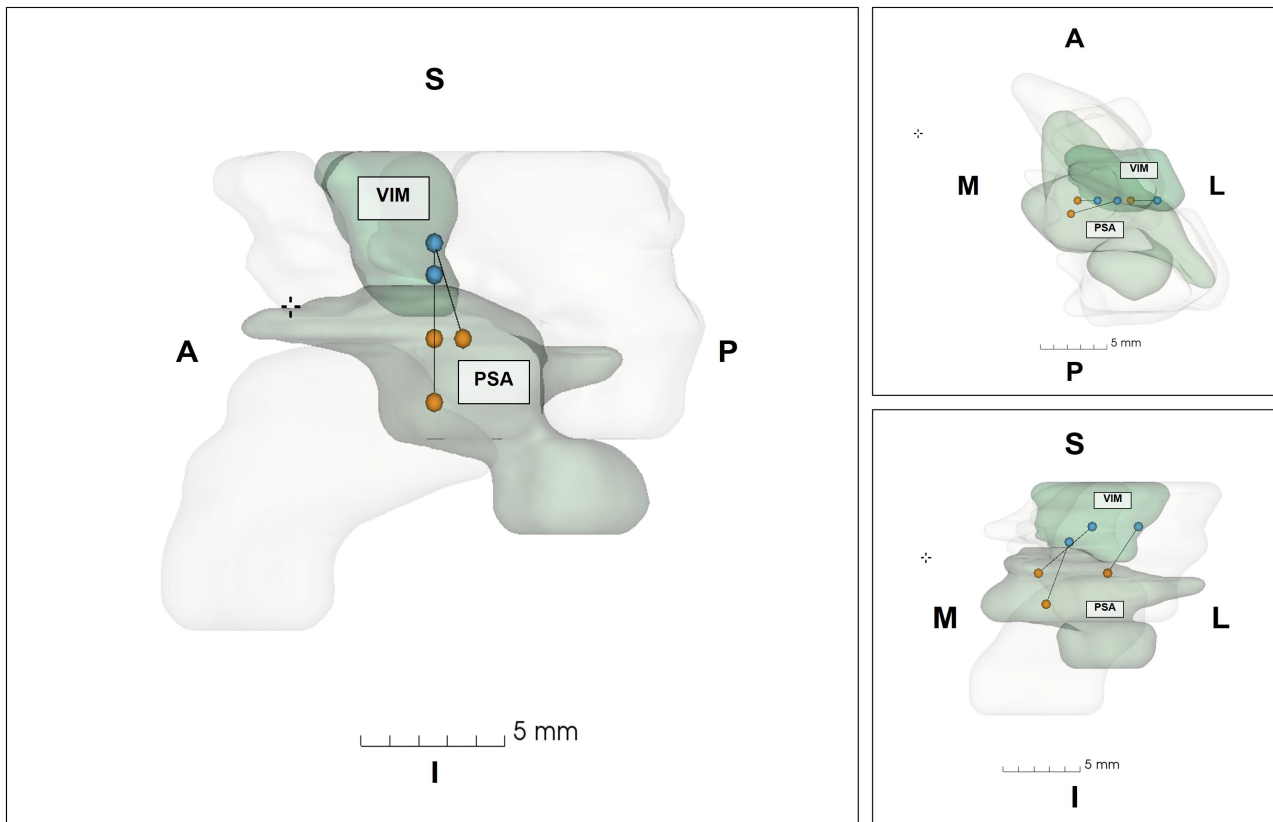


FIGURE 2: Visual representation of the vector of movement for 3 patients who received treatment at multiple targets and reported experiencing no illusion in one target and an illusion in another. Orange indicates targets evoking an illusion of self-motion in the posterior subthalamic area (PSA). Blue indicates targets not evoking any illusion in the nucleus ventralis intermedius of the thalamus (VIM). Black indicates the vector of movement, which clearly shows how moving inferiorly evoked an illusion of self-motion in these 3 patients. A = anterior; I = inferior; L = lateral; M = medial; P = posterior; S = superior.

regardless of whether they were located in the VIM or PSA. We calculated the average target for each axis for each group and visualized the results in Supplementary Materials, Figure S2. A statistically significant difference along the z-axis was again noted, with targets evoking an illusion of self-motion located more inferiorly (no movement: 0.83 ± 1.33 , movement: 0.03 ± 1.63 ; $t = 2.018$, $p = 0.048$). No statistically significant difference was noted along the x-axis (no movement: 15.22 ± 1.65 , movement: 14.55 ± 1.93 ; $t = 1.400$; $p = 0.167$) and y-axis (no movement: -5.04 ± 1.25 , movement: -5.09 ± 0.96 ; $t = 0.173$, $p = 0.863$).

Finally, we investigated whether any difference in target location was present between sonications evoking a translational, rotational, and a mixed rotational/translational illusory self-motion, respectively (see Supplementary Materials, Table S4). No significant difference between groups was noted (x: $F = 0.501$, $p = 0.609$; y: $F = 0.529$, $p = 0.592$; z: $F = 1.051$, $p = 0.356$). Nor were statistically significant differences noted by comparing targets based on the specific rotational movement evoked, namely pitch, roll, yaw, and a combination of the

previous movements (see Supplementary Materials, Table S5; x: $F = 0.323$, $p = 0.862$; y: $F = 1.737$, $p = 0.147$; z: $F = 0.757$, $p = 0.555$).

Binary Logistic Regression Analysis for Illusion of Movement

We performed a binary logistic regression analysis to estimate the ORs for experiencing illusory self-motion. We limited the selection of our independent variable to one MRgFUS parameter (power), whereas we categorized each sonication based on the z-axis coordinate, as being in VIM for coordinates above or on the AC-PC plane and in the PSA for coordinates below the AC-PC plane. Both being sonicated in the PSA (OR = 2.1, 95% confidence interval [CI] = 1.077–4.087, $p = 0.029$) and being sonicated at a higher power (OR = 4.0, 95% CI = 1.2–13.7, $p = 0.025$) were associated with higher odds of experiencing an illusion of self-motion (Supplementary Materials, Table S8). The overall accuracy of classification based on this model is 61.1% (specificity, 34.3%; sensitivity, 81.5%).

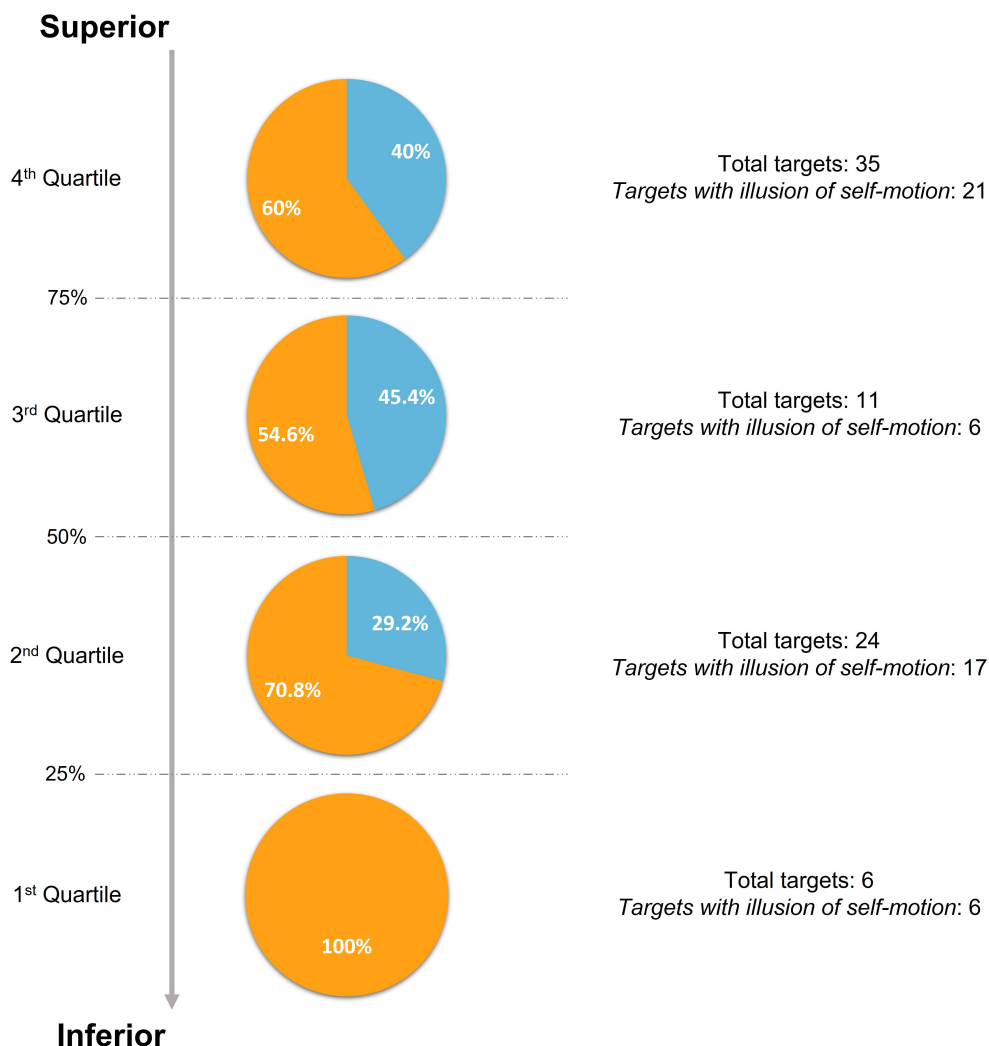


FIGURE 3: Sequential pie charts illustrating the distribution along the z-axis (in relative percentage) of sonications with (represented in orange) and without the illusion of self-motion (represented in blue) divided into quartiles of z-axis coordinates' distribution (1st quartile, <25%; 2nd quartile, ≥25% and <50%; 3rd quartile, ≥50% and <75%; 4th quartile, ≥75%). Inferior coordinates more frequently evoked an illusion of self-motion.

Discussion

In this study, we showed that 63% of patients in our cohort experienced an illusion of self-motion. Of cases with a sonication-induced illusion, 85% were pitch plane rotations, with the sensation of being tilted backward (76% pure pitch plane rotations). Rotational movements in other directions, and translational and combined rotational and translational movements were less frequently described. It is noteworthy that irrespective of whether the right or left VIM/PSA was sonicated, the illusion of self-movement was not lateralized.

We also reported that sonications that evoked an illusion of self-motion were located more inferiorly in the VIM/PSA and involved higher ultrasound power. The likelihood of experiencing such an illusion is 4 times higher for sonications at the higher power level versus the lower power level, and twice as likely for sonications

located inferiorly in the PSA versus those superiorly in the VIM.

Illusion of Self-Motion, Vestibular Network, and Magnetic Vestibular Stimulation

Subtyping illusions on the basis of self-motion characteristics, the commonest illusion was of a rotational movement. Most patients (approximately 84%) reported the sensation of being tilted backward in the pitch plane, whereas only a few reported spinning or tilting in the yaw or roll plane. Although this phenomenon has been reported previously,¹² the perception of being tilted along the pitch plane has never been documented in detail.

Previous neurophysiological studies in humans using microelectrode recordings have described how, when the VIM and the cerebellothalamic tract are electrically stimulated, vestibular responses are often experienced as a

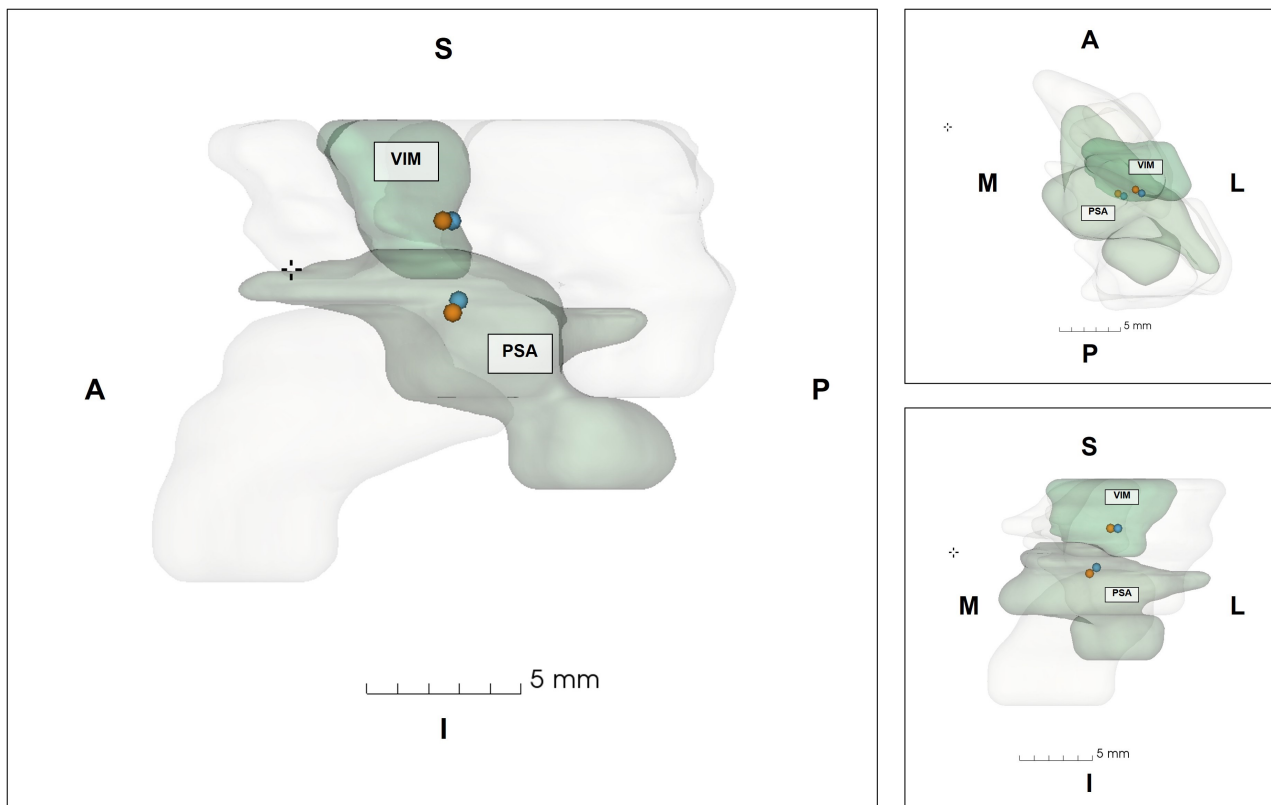


FIGURE 4: Visual representation of the nucleus ventralis intermedius of the thalamus (VIM) and posterior subthalamic area (PSA) targets. In the VIM, orange indicates targets evoking an illusion of self-motion; blue indicates targets not evoking any illusion. In the PSA, orange indicates targets evoking an illusion of self-motion; blue indicates targets not evoking any illusion. Targets evoking an illusion of self-motion in the PSA are located more inferiorly, medially, and anteriorly compared to “no-illusion” targets. In the VIM, targets with and without the illusion of self-motion overlap along the three axes. A = anterior; I = inferior; L = lateral; M = medial; P = posterior; S = superior.

sensation of movement through space.^{9,10} These illusions of self-motion can be categorized based upon the plane in which they occur and their relationship to the patient’s position. Examples of these classifications include not only rotations along a pitch plane, but also yaw and roll plane rotations, and sensations of rising or falling.⁹ These features, typical of activating vestibular circuits, provide a means to localize vestibular structures in the thalamus, brainstem, and along the fibers climbing from the brainstem to the thalamus.²¹ A map of the vestibular projections to the thalamus has been created, and these areas correspond to the human VIM⁹ and the cerebellothalamic tract.²¹ In addition to microelectrode recording, the interaction between DBS and the vestibular system has also been investigated, particularly with regard to motion perception. Shaikh and colleagues⁸ showed that stimulation of the vestibulothalamic pathway that passes in proximity to the subthalamic nucleus induces yaw plane rotational illusions of self-motion in patients with PD. Hence, it is likely that vestibular signaling is modulated via sonications along the cerebellothalamic tract in the VIM/PSA. In contrast, one explanation for targets not evoking an illusion,

which tend to be located more superiorly in the VIM, is that the cerebellothalamic fibers arborize as they ascend into the VIM, rendering them more diffuse. This potentially explains why illusions of self-motion are less predictable when linked to stimulation in this area.

The reported dizziness within strong static magnetic fields of MRI machines can be explained by the Lorentz force induced in the labyrinth of the inner ear due to the interaction of ionic currents and the magnetic field.²² In subjects with intact vestibular function, this force causes a constant horizontal/torsional nystagmus and a reported transient sense of rotation, primarily in the yaw plane.^{23,24} This perception typically subsides after few minutes. Mian and colleagues documented that 86% of subjects experienced rotation in roll and 36% in yaw (8% in pitch).²⁴ The perceptual adaptation (of dizziness) within the scanner indicates a differential perceptual and nystagmic response, otherwise known as perceptuoreflex uncoupling, which is mediated by a cerebellar mechanism.²⁵ Because ascending cerebellar pathways are involved in vestibular perception,^{26,27} one possibility for the illusory self-motion during MRgFUS is the sonication-induced disruption of

TABLE 3. Comparison of MRgFUS Power and Coordinates between Sonications with and without Illusion of self-motion in the VIM and PSA in the Prospective Cohort

MRgFUS Characteristics	VIM		PSA	
	No Illusion of Self-Motion	Illusion of Self-Motion	No Illusion of Self-Motion	Illusion of Self-Motion
MRgFUS parameters				
Power, W	599.73 (215.94)	627.65 (155.23)	586.37 (142.6)	603.0 (146.7)
Target coordinates				
x, mm	15.49 (1.59)	15.5 (1.64)	14.48 (1.69)	13.69 (1.47)
y, mm	−4.9 (1.33)	−4.89 (1.03)	−5.44 (0.96)	−5.18 (0.78)
z, mm	1.50 (0.83)	1.59 (0.8)	−0.99 (0.05)	−1.38 (0.72)*

Coordinates have been scaled to the averaged anterior commissure–posterior commissure line from our cohort of patients. Mean and standard deviation (in parentheses) are reported. A statistically significant difference (*) in target localization along the z-axis has been observed in the PSA ($t = 2.538$, $p = 0.018$).

PSA =posterior subthalamic area; MRgFUS = magnetic resonance imaging-guided focused ultrasound; VIM = ventralis intermedius.

vestibular perceptual signaling in ascending cerebellar thalamic circuits. This, being unilateral, may engender a bias in motion sensing pathways, provoking a vertiginous sensation, akin to that observed in some patients with acute cerebellar lesions.^{26,27} Notably, as compared with reports of healthy subjects during magnetic vestibular stimulation, most of our cases had a pitch plane sensation. Interestingly, during magnetic vestibular stimulation, patients with unilateral peripheral vestibular dysfunction manifest a strong vertical nystagmus in addition to the horizontal component.²⁸ This supports the notion that MRgFUS may result in functional unilateral vestibular pathway modulation, as this evokes a vertical plane illusion. Note, however, that unfortunately the perceptual response to the static magnetic field of patients with unilateral vestibular dysfunction has not been recorded.

In this scenario, experiencing the illusion of self-motion relies on several aspects, such as the strength of the magnetic field and its orientation relative to the head.^{22,23} These are 2 important MRI-related factors, which together with the MRgFUS parameters and the neuroanatomical location might explain why the illusion happens only in some patients and only during some sonications. Although this hypothesis is fascinating, it would be necessary to measure the effect of static head pitch on the illusion of self-motion and demonstrate that the motion perception during the MRgFUS sonication is associated with vertical nystagmus to validate it. Nevertheless, consistent with these findings, previous electrical stimulation of VIM reported yaw plane vertigo, which is the effect we predict when there is VIM stimulation/modulation outside of an MRI-related static magnetic field.

Illusion of Self-Motion and Postural Control

Another critical feature that has not been objectively assessed in patients undergoing functional stimulation of thalamic structures is the contribution of the vestibular system in postural imbalance. We posit that the vestibularly mediated postural control network and the vestibular motion perception network are intertwined, such that modulation of one network inevitably disrupts the other. Hence, experiencing an illusion of self-motion during MRgFUS likely implies the modulation of both motion perception and postural control networks by sonications of the VIM/PSA. This proposition finds support from both direct and indirect evidence. Neuroimaging studies have directly linked vestibular motion perception to vestibularly mediated postural function, highlighting the importance of temporo-occipital circuits.^{6,7} In addition, previous discussions support the involvement of the VIM in vestibular perception. Indirect evidence comes from VIM-DBS studies, revealing alterations in blood oxygen level-dependent signal activity in multisensory integration cortical regions (including the temporo-occipital regions and cerebellum),^{29,30} and reports of balance worsening in ET patients receiving VIM-DBS,^{31,32} likely due to vestibulocerebellar activation.³³ Finally, although we cannot entirely dismiss the possibility that the illusion of self-motion solely originates from interference in the vestibular perceptual network without perturbing the vestibularly mediated postural network, this scenario appears improbable.

It should be noted that patients' reports of illusory self-motion necessarily involve multisensory pathways integrating inputs from visual, vestibular, and

somatosensory information. This is reasonable given that virtually all higher order vestibular responsive neurons also respond to other sensory input.³⁴ At the level of the VIM, there are neurons responding to passive movements of joints and muscle compression of the contralateral hemibody both in animals and humans.^{35,36} In our cohort, the bilateral nature of the illusion of self-motion and the lack of proprioceptive loss following MRgFUS lesioning mitigate against the possibility of the illusion of self-motion being mediated by an isolated activation of the proprioceptive pathway, whereas a coactivation of vestibular and proprioceptive neurons within the VIM is plausible. The illusion of self-motion may arise from a perturbation of the information flow from the thalamus to the vestibular and somatosensory cortex, leading to an upstream transient failure to integrate somatosensory and vestibular information.

Alternative Explanations of the Illusion of Self-Motion

It is possible that the illusion of self-motion is evoked via the direct effects of ultrasound on otolithic receptors. This effect seems unlikely, as illusions of self-motion induced by skull vibration elicit yaw plane illusions and are frequently associated with malaise (including motion sickness).³⁷ Recent computational models have shown how the skull may potentially facilitate the propagation of shear waves to the ear, finally leading to activation of the inner ear organs. This may explain some of the off-target effects observed in low-intensity focused ultrasound neuromodulatory studies.³⁸ Nevertheless, it is true that the spatial localization of the MRgFUS target linked to the illusion of self-motion does not support indirect effects of MRgFUS.

Conclusions

In conclusion, we mapped vestibular–perceptual illusions provoked by MRgFUS in patients with ET and PD tremor. The mechanisms behind this phenomenon are uncertain, but likely involve the interplay between the modulation/stimulation exerted by the ultrasound and the effect of the static magnetic field on the vestibular system. By considering this interplay, the high spatial resolution, and the potential to create transient intraprocedural and short-term postprocedural symptoms, MRgFUS can be used as a tool to map the functions of small and deep brain structures, revealing spatial and functional organization of brain networks including the vestibular network. Considering the overlap between the motion perception and the postural control networks, MRgFUS might be used to investigate and treat patients with balance problems by means of modulating key structures previously

identified by evoking an illusion of self-motion while the patient is in the MRI scanner.

Acknowledgments

No funding was received for this work. Y.T. and B.M.S. are supported by the MRC and Moulton Foundation. B. M.S. is supported by the Imperial NIHR Biomedical Research Centre, Imperial Health Charity, US Department of Defense, and UK Ministry of Defense.

Author Contributions

M.C., P.B., and B.M.S. contributed to conception and design of the study. M.C., B.M.S., A.J., N.Y., J.S., S.A., and P.B. contributed to acquisition and analysis of data. All authors contributed to drafting the text or preparing the figures.

Potential Conflicts of Interest

Nothing to report.

Data Availability

The authors confirm that the data supporting the findings of this study are available within the article and its supplementary material.

References

1. Binder DK, Shah BB, Elias WJ. Focused ultrasound and other lesioning in the treatment of tremor. *J Neurol Sci* 2022;435:120193.
2. Natera-Villalba E, Matarazzo M, Martinez-Fernandez R. Update in the clinical application of focused ultrasound. *Curr Opin Neurol* 2022;35: 525–535.
3. Kirsch V, Keeser D, Hergenroeder T, et al. Structural and functional connectivity mapping of the vestibular circuitry from human brainstem to cortex. *Brain Struct Funct* 2016;221:1291–1308.
4. Barmack NH. Central vestibular system: vestibular nuclei and posterior cerebellum. *Brain Res Bull* 2003;60:511–541.
5. Cullen KE, Taube JS. Our sense of direction: progress, controversies and challenges. *Nat Neurosci* 2017;20:1465–1473.
6. Hadi Z, Mahmud M, Pondeca Y, et al. The human brain networks mediating the vestibular sensation of self-motion. *J Neurol Sci* 2022; 443:120458.
7. Calzolari E, Chepishcheva M, Smith RM, et al. Vestibular agnosia in traumatic brain injury and its link to imbalance. *Brain* 2021;144: 128–143.
8. Shaikh AG, Straumann D, Palla A. Motion illusion-evidence towards human vestibulo-thalamic projections. *Cerebellum* 2017;16:656–663.
9. Hawrylyshyn PA, Rubin AM, Tasker RR, et al. Vestibulothalamic projections in man: a sixth primary sensory pathway. *J Neurophysiol* 1978;41:394–401.
10. Tasker RR, Organ LW, Hawrylyshyn P. Sensory organization of the human thalamus. *Appl Neurophysiol* 1976;39:139–153.
11. Jameel A, Gedroyc W, Nandi D, et al. Double lesion MRgFUS treatment of essential tremor targeting the thalamus and posterior sub-

- thalamic area: preliminary study with two year follow-up. *Br J Neurosurg* 2022;36:241–250.
12. Elias WJ, Huss D, Voss T, et al. A pilot study of focused ultrasound thalamotomy for essential tremor. *N Engl J Med* 2013;369:640–648.
 13. Elias WJ, Lipsman N, Ondo WG, et al. A randomized trial of focused ultrasound thalamotomy for essential tremor. *N Engl J Med* 2016; 375:730–739.
 14. Bond AE, Shah BB, Huss DS, et al. Safety and efficacy of focused ultrasound thalamotomy for patients with medication-refractory, tremor-dominant Parkinson disease: a randomized clinical trial. *JAMA Neurol* 2017;74:1412–1418.
 15. Zaaroor MSA, Goldsher D, Eran A, et al. Magnetic resonance-guided focused ultrasound thalamotomy for tremor: a report of 30 Parkinson's disease and essential tremor cases. *J Neurosurg* 2018; 128:202–210.
 16. Fishman PS, Elias WJ, Ghanouni P, et al. Neurological adverse event profile of magnetic resonance imaging-guided focused ultrasound thalamotomy for essential tremor. *Mov Disord* 2018;33:843–847.
 17. Kahane P, Hoffmann D, Minotti L, Berthoz A. Reappraisal of the human vestibular cortex by cortical electrical stimulation study. *Ann Neurol* 2003;54:615–624.
 18. Segar DJ, Lak AM, Lee S, et al. Lesion location and lesion creation affect outcomes after focused ultrasound thalamotomy. *Brain* 2021; 144:3089–3100.
 19. Schaltenbrand G, Wahren W. *Atlas for Stereotaxy of the human brain*. Stuttgart: Thieme, 1977.
 20. Fedorov A, Beichel R, Kalpathy-Cramer J, et al. 3D slicer as an image computing platform for the quantitative imaging network. *Magn Reson Imaging* 2012;30:1323–1341.
 21. Gallay MN, Jeanmonod D, Liu J, Morel A. Human pallidothalamic and cerebellothalamic tracts: anatomical basis for functional stereotactic neurosurgery. *Brain Struct Funct* 2008;212:443–463.
 22. Ward BK, Roberts DC, Otero-Millan J, Zee DS. A decade of magnetic vestibular stimulation: from serendipity to physics to the clinic. *J Neurophysiol* 2019;121:2013–2019.
 23. Mian OS, Li Y, Antunes A, et al. Effect of head pitch and roll orientations on magnetically induced vertigo. *J Physiol* 2016;594:1051–1067.
 24. Mian OS, Li Y, Antunes A, et al. On the vertigo due to static magnetic fields. *PLoS One* 2013;8:e78748.
 25. Nigmatullina Y, Hellyer PJ, Nachev P, et al. The neuroanatomical correlates of training-related perceptuo-reflex uncoupling in dancers. *Cereb Cortex* 2015;25:554–562.
 26. Shaikh AG, Palla A, Marti S, et al. Role of cerebellum in motion perception and vestibulo-ocular reflex-similarities and disparities. *Cerebellum* 2013;12:97–107.
 27. Seemungal BM, Bronstein AM. A practical approach to acute vertigo. *Pract Neurol* 2008;8:211–221.
 28. Ward BK, Roberts DC, Della Santina CC, et al. Magnetic vestibular stimulation in subjects with unilateral labyrinthine disorders. *Front Neurol* 2014;5:28.
 29. Ceballos-Baumann AO, Boecker H, Fogel W, et al. Thalamic stimulation for essential tremor activates motor and deactivates vestibular cortex. *Neurology* 2001;56:1347–1354.
 30. Deiber MP, Pollak P, Passingham R, et al. Thalamic stimulation and suppression of parkinsonian tremor. Evidence of a cerebellar deactivation using positron emission tomography. *Brain* 1993;116: 267–279.
 31. Fasano A, Herzog J, Raethjen J, et al. Gait ataxia in essential tremor is differentially modulated by thalamic stimulation. *Brain* 2010;133: 3635–3648.
 32. Reich MM, Brumberg J, Pozzi NG, et al. Progressive gait ataxia following deep brain stimulation for essential tremor: adverse effect or lack of efficacy? *Brain* 2016;139:2948–2956.
 33. Liu J, Wang LN. Mitochondrial enhancement for neurodegenerative movement disorders: a systematic review of trials involving creatine, coenzyme Q10, idebenone and mitoquinone. *CNS Drugs* 2014;28: 63–68.
 34. Dieterich M, Brandt T. The parietal lobe and the vestibular system. *Handb Clin Neurol* 2018;151:119–140.
 35. Liedgren SR, Schwarz DW. Vestibular evoked potentials in thalamus and basal ganglia of the squirrel monkey (*Saimiri sciureus*). *Acta Otolaryngol* 1976;81:73–82.
 36. Ohye C, Narabayashi H. Physiological study of presumed ventralis intermedialis neurons in the human thalamus. *J Neurosurg* 1979;50: 290–297.
 37. Lackner JR, Graybiel A. Elicitation of vestibular side effects by regional vibration of the head. *Aerosp Med* 1974;45:1267–1272.
 38. Salahshoor H, Shapiro MG, Ortiz M. Transcranial focused ultrasound generates skull-conducted shear waves: computational model and implications for neuromodulation. *Appl Phys Lett* 2020;117:033702.